Available free online at www.medjchem.com

Mediterranean Journal of Chemistry *Mediterranean Journal of Chemistry* **2024**, 14(2), 112-121

Aluminum and Mild Steel Inhibition Investigation Using Trithiocyanuric Acid: Insights from Density Functional Theory (DFT)

Fater Iorhuna *, [1], Abdullahi Muhammad Ayuba [1], Thomas Aondofa Nyijime [2], and Saifullahi Lawal Muhammad [3]

[1]*Department of Pure and Industrial Chemistry, Faculty of Physical Sciences, Bayero University, PMB 3011, Kano, Nigeria*

[2]*Department of Chemistry, Joseph Sawuan Tarka University, Makurdi, Benue, Nigeria*

[3]*Chemistry Department Federal University Gashua, Yobe, Nigeria*

Abstract: The study investigates the corrosion inhibition properties of Trithiocyanuric Acid (TTCA) on Aluminum and mild steel using Density Functional Theory (DFT) and Molecular Dynamics (MD) simulations. The electronic properties of TTCA, including the highest occupied molecular orbital (E_{HOMO}) of -7.617 eV and the lowest unoccupied molecular orbital (E_{LUMO}) of -4.301 eV, yield an energy gap of 3.316 eV. The calculated absolute electronegativity was 5.959 eV, global hardness obtained was 1.658 eV, global softness was 0.603136 eV, global electrophilicity index was 1.449891 eV, and nucleophilicity was 0.689707 eV. The energy of back donation was also 0.689707 eV. The charge transfer parameters, ΔNFe and ΔNAl, are also 0.862989 eV and -0.21653 eV, respectively, indicating effective interaction with both metal surfaces. Functional groups in TTCA contribute significantly to its corrosion inhibition performance by facilitating alignment on the metal surfaces. The interaction mechanism is characterized as physisorption, with binding energy values falling within the range typical for this adsorption type. The results suggest that TTCA is a suitable corrosion inhibitor for Aluminum and mild steel, making it a promising molecule for industrial applications where metal protection is essential.

Keywords: Trithiocyanuric Acid; Aluminum; DFT; Mild steel.

1. Introduction

Corrosion inhibitors are compounds that can physically, chemically, or both adsorb into the metal/solution system. This adsorption technique successfully shields the metal from direct exposure to corrosive acidic solution [1]. Heteratoms with lone pairs electrons, including phosphorus, oxygen, sulfur, and selenium, provide this protection. At the heteroatom molecules, which are much on the metal surface containing several metal atoms, these atoms interact with the metal surface in an acidic environment to form complexes with inhibitor [2]. Corrosion is a common occurrence that presents severe difficulties for many construction and oil industries, resulting in significant financial losses and safety issues. Due to their favorable mechanical qualities and affordability, mild steel and Aluminum are two metals prone to corrosion and are often used in various applications [3]. However, their vulnerability to corrosion needs the development of efficient inhibitors and corrosion inhibition techniques to limit the negative consequences.

Trithiocyanuric acid (TTCA), presented in Fig.1 is a heterocyclic compound containing three thiocyanate groups, shows promising potential, having many functional groups as well as the presence of pi-bond in the structure and hetero-atoms in the structure as a corrosion inhibitor [4]. The presence of multiple thiol (-SH) groups, precisely three per molecule, suggested the molecule could be a potent inhibitor on metallic surfaces. The thiol group is highly reactive towards metal surfaces, forming coordination bonds with metal ions and effectively adsorbing onto the surface. The thiol groups' chelating ability on the metal can form stable complexes with metal ions that can inhibit corrosion by blocking active sites on metal surfaces: Aluminium and Iron [2].

Traditional experimental approaches, such as those from Hong *et al.* [5], offer valuable insights into corrosion inhibition. Hong et al. explore the inhibitory effect of trithiocyanuric acid on copper corrosion in 3.0 wt.% NaCl. Similarly, Chen *et al.* [6] investigated the corrosion inhibition of copper in hydrochloric acid using trithiocyanuric acid but cannot often elucidate

**Corresponding author: Fater Iorhuna*
Email address: uyerfater@gmail.com
DOI: http://dx.doi.org/10.13171/mjc02407171793iorhuna

Received May20, 2024
Accepted June 22, 2024
Published July 17, 2024

the intricate molecular interactions that determine inhibitor effectiveness [7]. Additionally, the study focuses solely on a single metal, copper. Computational methods such as density functional theory (DFT) were needed to complement experimental studies and provide detailed molecular insights into the corrosion inhibition process.

The present study will use computational methods such as Density Functional Theory (DFT) and simulation methods to examine the inhibition mechanism of the molecule Trithiocyanuric acid (TTCA) on the surfaces of Al(110) and Fe(110).

Density functional theory (DFT) and simulation methods offer a powerful means to investigate the interaction between corrosion inhibitors like TTCA and metal surfaces at the atomic level. By employing DFT calculations and molecular dynamics simulations, it is hypothesized that the adsorption behavior of TTCA on Aluminum and mild steel surfaces can be elucidated, providing valuable information about the stability and effectiveness of the inhibitor-metal complexes.

Moreover, it is anticipated that DFT calculations can offer insights into the electronic structure and bonding characteristics of TTCA-metal complexes, aiding in designing and optimizing novel corrosion inhibitors with enhanced performances. Molecular dynamics simulations can further complement these findings by providing information regarding the dynamics and stability of the inhibitor-metal interface under varying environmental conditions.

However, it is essential to acknowledge the limitations of DFT and simulation methods when studying corrosion inhibition processes. Firstly, the accuracy of DFT calculations heavily relies on the choice of exchange-correlation functional and basis sets, which may introduce uncertainties in the calculated properties [8-11].

But, DFT calculations and simulations simplify the complexity of corrosion environments by reducing the time involved in the experimental method. The density functional theory calculation can provide insights into the electronic structure, binding energies, and reactivity of inhibitor molecules with metal complexes, which is often faster than experimental methods, which may require lengthy setup and analysis time. In addition, DFT can contribute to reducing the environmental impact of chemical experimentation and waste production [12-15]. This research is limited to the Density Functional Theory (DFT) and simulation of the molecule Trithiocyanuric Acid (TTCA) on Aluminum and mild steel.

2. Experimental

Quantum chemical calculations were conducted using the DMol3 module within the BIOVIA Material Studio 8.0 program (Accelrys, Inc.), employing the underlying Density Functional Theory (DFT) principles. The B3LYP function was applied to compute the parameters, utilizing a basis set of "double-numeric polarization" (DNP) in the gas phase model [16-18]. The calculation encompassed determining the Frontier energies of the molecule **TTCA** with equations 1-11 following the extended Koopman's theorem [19]. These equations elucidate the initial electron distribution in the molecule and the computation of local reactivity, specifically the Fukui function f(r), through ab-initio quantum chemistry methods [20]. Before establishing their stable geometry, the molecules were drawn using Chem Draw Ultra 7.0.3 by Cambridge Software [21].

IE: Ionization energy (eV) $IE = -E_{HOMO}$ (1)

AE: Electron affinity (eV) $AE = -E_{LUMO}$ (2)

ΔE_g: Energy gap (eV) $\Delta E_g = E_{LUMO} - E_{HOMO}$ (3)

χ: absolute electronegativity (eV)

$$\chi = \frac{IE+AE}{2} = -\frac{(E_{HOMO}+E_{LUMO})}{2} \quad (4)$$

η: global hardness (eV) $\eta = \frac{IE-AE}{2} = \frac{(E_{LUMO}-E_{HOMO})}{2}$ (5)

σ: global softness $(eV)^{-1}$ $\boldsymbol{\sigma} = \frac{1}{\eta} = -\frac{2}{E_{HOMO}-E_{LUMO}}$ (6)

ω: global electrophilicity index (eV) $\boldsymbol{\omega} = \frac{\mu^2}{2\eta} = \frac{\chi^2}{2\eta}$ (7)

μ: chemical potential (Debye) $\mu \approx -\frac{1}{2}(IE+AE) = \frac{1}{2}(E_{LUMO}+E_{HOMO})$ (8)

ε: nucleophilicity $(eV)^{-1}$ $\boldsymbol{\varepsilon} = \frac{1}{\omega}$ (9)

ΔE_{b-d}: Energy of back donation $\Delta \boldsymbol{E}_{b-d} = -\frac{\eta}{4} = \frac{1}{8}(E_{HOMO} - E_{LUMO})$ (10)

ΔN: Fraction of electron(s) transfer $\Delta N = \frac{\chi metal - \chi Inh.}{2(\eta metal + \eta Inh)}$ (11)

The inhibitor molecule's absolute hardness, denoted as ηinh, and absolute electronegativity, represented by χinh, are comparable to Fe and Al. In theory, the global hardness of iron and Aluminium surfaces is 0 eV, and the electronegativity of bulk iron and Aluminum are χFe = 7.0 eV and χAl=,5.6eV assuming a higher density for metallic bulk compared to neutral metallic atoms [22–24]. The distinction between nucleophilic and electrophilic local Fukui functions lies in the definition of the Fukui second function (f^2), also referred to as the dual descriptor Δf(k). Based on the Fukui behavior of atoms, these functions determine the electrophilicity or nucleophilicity of molecules [25]. If $f^2 > 0$, site k favors a nucleophilic attack, whereas if $f^2 < 0$, site k favors an electrophilic attack. Thus, f^2 is a selectivity index for determining whether attacks are electrophilic or nucleophilic.

$$\boldsymbol{f(k)^{+}} = \boldsymbol{qk(N+1) - qk(N)} \text{ (for nucleophilic attack)} \quad (12)$$

$$\boldsymbol{f(k)^{-}} = \boldsymbol{qk(N) - qk(N-1)} \text{(for electrophilic attack)} \quad (13)$$

$$\boldsymbol{f}(\mathrm{k})^{0} = \frac{\boldsymbol{qk(N+1)-qk(N-1)}}{\boldsymbol{2}} \text{ (for radical attack)} \quad (14)$$

$$\boldsymbol{\Delta f(k) = f^{+}\text{-}f^{-} = f^{2}} \quad \text{Fukui function)} \quad (15)$$

In this context, N represents the total number of electrons in the molecule. At the same time, N+1 denotes an anion formed by adding an electron to the Lowest Unoccupied Molecular Orbital (LUMO) of the neutral molecule, and N-1 signifies a cat ion formed by removing an electron from the Highest Occupied Molecular Orbital (HOMO) of the neutral molecule. The variable qk represents the net charge of atom k within the molecule, reflecting the electron density at a specific point r in space surrounding the molecule. The initial ground state geometry was utilized as the reference point for all subsequent calculations. Employing an atomic charge partitioning method, such as Mulliken population analysis outlined in Equations, these functions were concentrated on the nuclei of the atoms [26-27].

Molecular Dynamic Simulations

A quench adsorption method known for its high stability was employed to mimic the behavior of the TTCA molecule on closely packed surfaces of Fe (110), Al (110) atoms. This simulation was conducted using the FORCITE tool package integrated into the BIOVIA Materials Studio 8.0 software (Accelrys, Inc.). The simulation employed the COMPASS force field tool and the Smart algorithm approach within a simulation box measuring 17Å x 12Å x 28Å, aiming to model a representative surface area [28]. The Fe and Al crystals were cleaved along the (110) planes at a fractional depth of 3.0 Å, and the form of the bottom layers was fixed before surface optimization to mitigate edge effects stemming from molecular sizes. A 3x3 supercell was then generated by extending the surfaces. Maintaining a temperature of 350K struck a balance between excessive kinetic energy causing molecule desorption and insufficient kinetic energy hindering molecule movement across the surface [13,23]. The simulation, conducted over 5 ps with a time step of 1 fs, employed the NVT (microcanonical) ensemble to control temperature. The quenching occurred every 250 steps for a total of 5000 cycles to ensure statistical accuracy of energy values on the examined Fe and Al crystal surfaces. Utilizing FORCITE, the lowest energy interactions between molecules and metal surfaces were determined through geometry optimization [3,4,10,14,23].

Equations (16-17) were utilized to calculate the adsorption and binding energies of the TTCA - Metal-surface.

$$E_A = E_T - (E_I + E_S) \quad (16)$$

$$E_B = - E_A \quad (17)$$

Where E_A is the adsorption energy, E_T is the combined energy of the molecule and the metal surface, E_S is the energy of the metal surface, E_I is the energy of the inhibitor molecule without the iron surface, and E_B is the binding energy [23,29].

Chemical structures

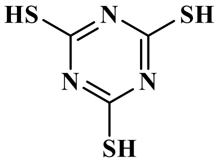

Figure 1. The structure of Trithiocyanuric Acid

3. Results and Discussion

HOMO (Highest Occupied Molecular Orbital: This refers to the highest energy molecular orbital that is occupied with electrons in a molecule. It represents the highest energy level at which electrons are found in a stable (ground state) molecule. The electrons in the HOMO are the ones involved in chemical reactions, particularly in donating electrons during bond formation. The lowest energy level at which an electron can be accepted to form a bond with another atom or molecule is referred to as the HOMO (Occupied Molecular Orbital) [30]. In corrosion studies, a molecule with a HOMO energy level matching or close to the energy of the unoccupied d-orbitals of metal ions can effectively coordinate with these ions, forming stable complexes. This coordination inhibits the electrochemical reactions responsible for corrosion by blocking the metal surface of corrosive prompt areas on the metal surface [10,21,30]. Therefore, understanding and optimizing the HOMO energy of inhibitor molecules is crucial in designing effective corrosion inhibitors for various metal systems.

Electrons in the LUMO are involved in accepting electrons during bond formation. The energy difference between -the HOMO and LUMO is important in understanding the reactivity and stability of molecules [31-32]. It's often referred to as the HOMO-LUMO gap. Smaller HOMO-LUMO gaps typically indicate higher reactivity, suggesting that electrons can more easily transit between the two orbitals, facilitating chemical reactions. Conversely, larger HOMO-LUMO gaps suggest greater stability, as it takes more energy to promote an electron from the HOMO to the LUMO. From the molecule TTCA studied on the Aluminum and mild steel surfaces, the E_{HOMO} of the molecule is -7.617eV, E_{LUMO} -4.301eV, which is why the HOMO-LUMO gap was 3.316eV. The result of the molecule was equivalent to the values obtained by Zarrouk *et al.*, Oyeneyin *et al.*, Iorhuna *et al.* [33-35].

Table 1. The energy parameter of the molecule TCCA

E-HOMO	-7.617
E-LUMO	-4.301
IE: Ionization energy (eV) IE	7.617
AE: Electron affinity (eV)	4.301
ΔE_g: Energy gap (eV) ΔE_g	3.316
χ: absolute electronegativity (eV)	5.959
η: global hardness (eV)	1.658
σ: global softness $(eV)^{-1}$	0.603
ω: global electrophilicity index (eV	1.449
ε :nucleophilicity	0.689
ΔE_{b-d}: Energy of back donation	-0.414
ΔNFe: Fraction of electron(s) transfer	0.863
ΔNAl: Fraction of electron(s) transfer	-0.216

According to Hadisaputra *et al.*, Jamil *et al.*, and Kokalj *et al.* [36-38], Inhibitors with high ionization energies(*I*) are less reactive, forming stable, protective layers on metal surfaces and reducing corrosion. On the other hand, the low ionization potential (*I*) indicates the ease with which the atom can release its outer electron. It can donate electrons to the metal surface, thus increasing corrosion inhibition efficiency [39]. In Table 1, the molecule TTCA has an Ionization energy of 7.617eV; this, according to moderately high ionization energy, ensures stable adsorption of inhibitors on metals. Meanwhile, inhibitors with high electron affinity can effectively accept electrons from metal surfaces, forming strong bonds and creating a protective barrier against corrosion. These inhibitors form stable complexes with metals, enhancing corrosion resistance [40]. High Absolute electronegativity (χ) values in Table 1 indicate that organic corrosion inhibitors are electron acceptors, while those with lower values indicate corrosion inhibitors as electron donors. The Absolute electronegativity value of TTCA was recorded as 5.959eV in Table 1. This is because corrosion inhibitors with low electronegativity values will make donating electrons easier or more reactive [41]. A higher global hardness (η) in Table 1 has the potential of having more stability on the surface and the molecule being reactive. Corrosion inhibitors with high global hardness are less likely to participate in chemical reactions that could degrade the inhibitor layer, thus providing better protection to the metal surface. Softer molecules are more reactive and can readily form bonds with metal surfaces, aiding adsorption. Therefore, an optimal balance between hardness and softness is crucial for effective corrosion inhibition [42]. Fraction of electron transfer (ΔN) represents the extent to which electrons are transferred between the inhibitor and the metal surface. A value of 0.862989 eV and -0.21653eV on Al and Fe indicates substantial electron transfer, suggesting strong interaction and bonding between the inhibitor and the metal. This enhances the stability of the protective layer, making it more effective in preventing corrosion. The molecule TTCA has a high Fraction of electron transfer on Al and less on Fe. The values of the Fraction of electron transfer suggest good interaction with the metal surface, potentially balanced by appropriate softness to facilitate adsorption [43-44]. In the context of corrosion inhibition, a higher electrophilicity index (ω) means the molecule can effectively accept electrons from the metal, forming a stable protective layer [45]. This protective layer prevents further oxidation of the metal, thus inhibiting corrosion. The TTCA properties suggest moderate electrophilicity, contributing to its corrosion inhibitor effectiveness [46]. In corrosion inhibition, nucleophilic property electrons to the metal surface, forming bonds that create a protective layer. TTCA molecule, with its high Fraction of electron transfer, likely exhibits significant nucleophilicity, enhancing its ability to interact with the metal surface and form a protective barrier. A negative value, such as -0.4145 eV in the given molecule, indicates that the molecule can accept electron density from the metal, stabilizing the interaction and forming a protective layer [47-48]. This back donation mechanism is crucial for reinforcing the inhibitor's adherence to the metal surface and enhancing its protective qualities. Fig. 2 presents the optimized molecule, HOMO orbital, LUMO orbital, and the Density of the molecule. From the optimized molecule of the molecule presented in Fig. 2, the white, blue, grey, and yellow atoms represent Hydrogen, Nitrogen, Carbon, and Sulphur, respectively.

Optimized Geometry	**HOMO**	**LUMO**	**Electron density**
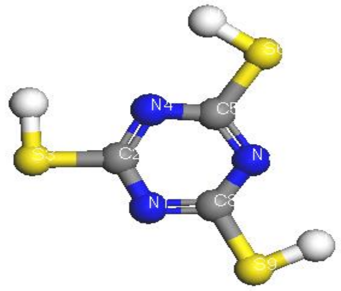	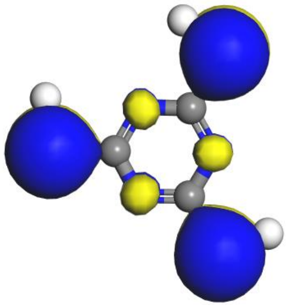	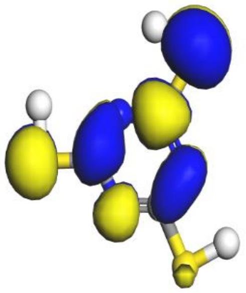	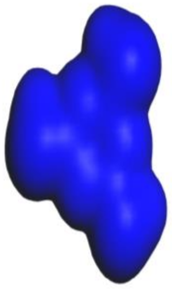

Figure 2. Optimized, HOMO, LUMO, and Density Orbitals of the molecule TTCA.

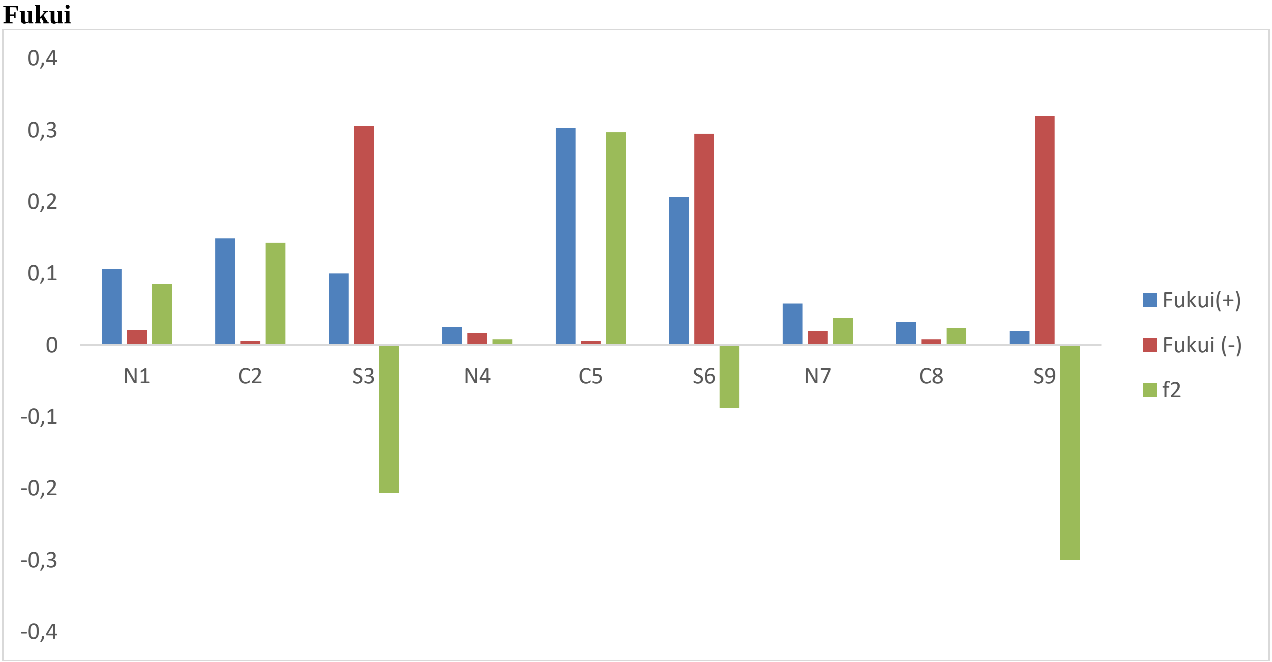

Figure 3. The Fukui functions of the molecule TTCA

The Fukui indices describe the local reactive sites of an organic system susceptible to nucleophilic or electrophilic attacks. Table 1 indicates the Fukui indices (f+, f−) of the molecule TTCA [28]. Large values of the Fukui indices (f+ and f−) Indicate molecular softness and chemically reactive sites [29,39].

The condensed Fukui dual descriptor (Δf) is presented in Table 1, which describes the atoms of the molecule that are susceptible to Electrophilic or nucleophilic attacks. The condensed Fukui dual descriptor (Δf) is a more explicit and accurate parameter than f+ and f− for describing local reactivity [30]. Atoms with positive Δf are susceptible to electrophilic attack, while those with negative Δf are susceptible to nucleophilic attack [31,40]. For the result presented in Fig. 3 only S3, S6 and S9 are negative while C2, N1, N4, C5, N7 and C8 are positive. As a result, a higher percentage of the molecule is susceptible to electrophilic attack than nucleophilic attack.

Bond length directly impacts inhibitor molecules' structural and electronic properties; its influence on corrosion inhibition effectiveness is indirect but significant. In their corrosion investigation, Iorhuna et al. Belghiti et al. consider bond length alongside other molecular characteristics to design inhibitors with optimal adsorption, electronic structure, chemical reactivity, and stability on metal surfaces under corrosive conditions. Thus, understanding the relationship between bond length and corrosion inhibition helps develop more effective and durable inhibitors for practical applications in metal protection [11,45]. Table 2 presents the bond length of the molecule before and after the simulation, which demonstrates how the bonds of the molecule behave before the corrosion inhibition of the surfaces and after the corrosion inhibition. From the result obtained, the bonds significantly affect the corrosion inhibition of the molecule, where the difference between before and after corrosion is recorded in Table 2.

Table 2. Bond length before and after simulation.

Bond Type	Bond Length Before((Angstroms)	Bond Length After((Angstroms)	Difference in bond length (Angstroms)
N1-C2	1.301	1.3	0.001
C2-S3	1.371	1.373	-0.002
C2=N4	1.715	1.716	-0.001
N4-C5	1.372	1.377	-0.005
C5-S6	1.371	1.372	-0.001
C5=N7	1.716	1.715	0.001
N7-C8	1.37	1.375	-0.005
C8-S9	1.372	1.371	0.001
N1-C8	1.714	1.714	0

Table 3. The bond angle between the atoms before and after simulation.

Angle Type	Bond Angle Before (Degree)	Bond Angle After (Degree)	Difference (Degree)
N1-C2-S3	115.989	115.980	0.009
N4=C2-S3	124.922	124.923	-0.001
C2=N4-C5	115.379	115.375	0.004
N4-C5-S6	119.164	119.165	-0.001
C5-S6=N7	124.646	124.643	0.003
C5=N7-C8	114.789	114.784	0.005
N7-C8-N1	116.142	116.141	0.001
N1-C8-S9	115.989	115.986	0.003
C2-N1-C8	124.922	124.924	-0.002

Bond angles can influence the distribution of electron density within the inhibitor molecule. This distribution affects the molecule's ability to donate or accept electrons, essential for forming bonds with metal atoms or ions on the surface [42,43]. Effective corrosion inhibitors often have specific electronic configurations that facilitate the formation of stable complexes with metal surfaces. Table 3 demonstrates the molecule's behavior regarding the angle between the bonded atoms. According to Belghiti *et al.*, the result obtained shows that the calculated bond angles for the inhibitor is planar; hence, the angle between link atoms tends to ±180° or ±0° from the result, the compound is expected to exhibit sp^2 hybridization with a lot of p-orbital character on the surfaces of Al(110) and Fe(110) [45]. The difference in the bond angle demonstrates that the molecule was influential in the corrosion inhibition of both Fe (110) and Al (110).

Molecular Dynamic Simulation

Table 4. The Energy parameter of the molecule after simulation on Al, and Fe surfaces

Properties	Fe(110)- TTCA	Al(110)- TTCA
Adsorption Energy (Kcalmol^{-1})	-25.59 ± 0.027	-20.51 ± 0.004
Total Energy of the Surface (Kcalmol^{-1})	0.000 ± 0.00	0.000 ± 0.00
Binding Energy (Kcalmol^{-1})	25.59 ± 0.027	20.51 ± 0.004

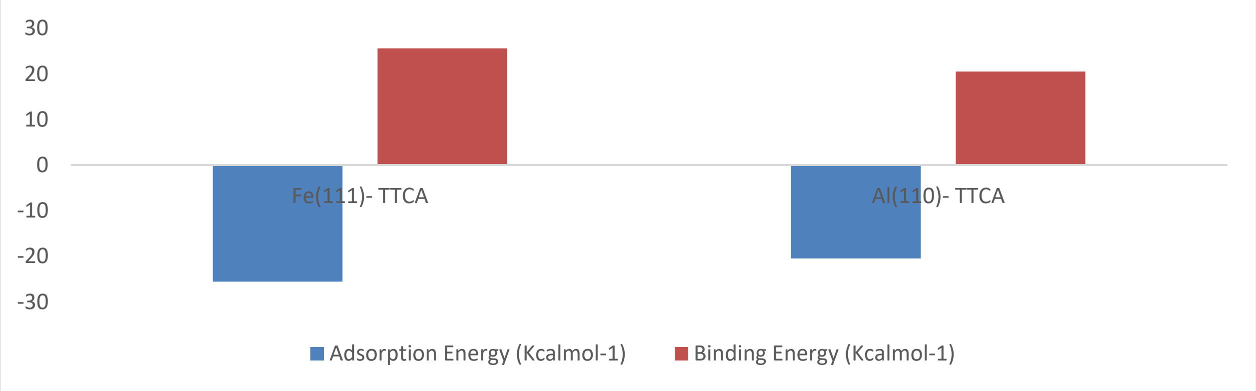

Figure 4. The graphical representation of the simulated energy difference.

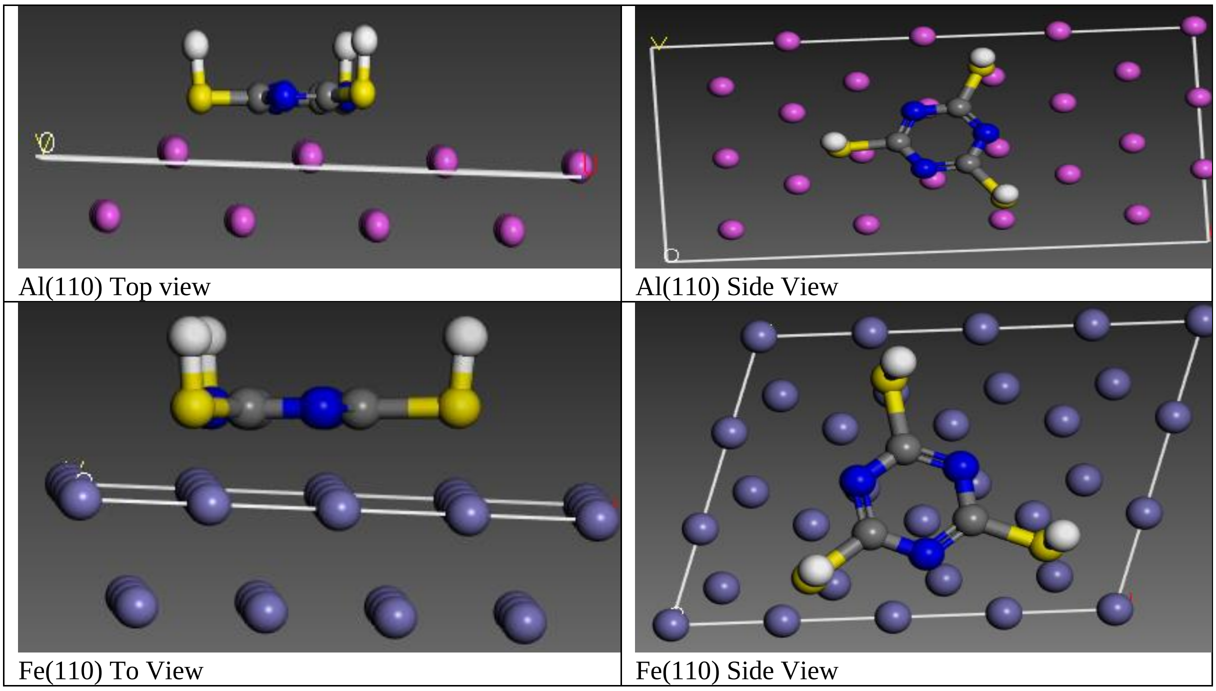
Al(110) Top view
Al(110) Side View
Fe(110) To View
Fe(110) Side View

Figure 5. The Molecule TTCA on the surfaces of the Al(110) and Fe(111)

Molecular Dynamic Simulation (MDS) provides a molecular-level insight into the interaction between inhibitors and metal surfaces, which is essential for investigations on corrosion inhibition. This computational method sheds light on the inhibitor molecules' dynamic behavior, how they adsorb onto metal surfaces, and how protective layers develop. MDS facilitates the creation of new inhibitors with improved qualities, clarifies the principles of corrosion inhibition, and allows the prediction of inhibition efficacy by modeling the atomic-scale motions and interactions. MDS is a potent instrument that may expedite the creation of efficient corrosion inhibitors, propelling progress in materials science and corrosion management tactics.

TTCA exhibits a notable binding affinity towards metal surfaces Fe(110) and Al(110), as evidenced by its binding energies of 25.59 kcal/mol on Fe(110) and 20.51 kcal/mol on Al(110), as demonstrated in

Table 4. This suggests strong adsorption capability, making TTCA a promising corrosion inhibitor for iron and aluminum substrates. The binding energy of 25.59 kcal/mol with Fe(110)- TTCA and 20.51 kcal/mol with Al(110)- TTCA suggests a relatively strong interaction between the adsorbate and the surface. High binding energy recorded by the molecule suggested a chemisorption rather than physisorption, which involves the formation of chemical bonds between the adsorbate and the surface atoms. . Fig. 4 compares the energy (Binding and Adsorption) value of the interaction on both surfaces graphically while Fig. 5 illustrates the interaction of the molecule TTCA with metal surfaces: Al(110)-TTCA and Fe(110)-TTCA. It describes how TTCA interacts with these surfaces and its alignment on them. This demonstration determines the molecule's effectiveness on the surface and also influences the molecule's binding energy.

4. Conclusion

From the electronic properties of TTCA, including the highest occupied molecular orbital (E_{HOMO}) of -7.617 eV and the lowest unoccupied molecular orbital (E_{LUMO}) of -4.301 eV, yielding an energy gap of 3.316 eV and the calculated absolute electronegativity 5.959 eV, global hardness 1.658 eV, global softness 0.603136 eV, global electrophilicity index 1.449891 eV, nucleophilicity 0.689707 eV and the charge transfer parameters, ΔN_{Fe} and ΔN_{Al}, 0.862989 eV and -0.21653 eV respectively. The effectiveness of these molecules as corrosion inhibitors stems from the functional groups, which facilitate the alignment on metal surfaces. This alignment supports physisorption as evidenced by binding energy values obtained from the typical interaction of the molecule with the system. These molecules demonstrate effective inhibition properties for Aluminum and iron, as presented in the research results.

- The molecule can be used effectively as a suitable inhibitor for Aluminum and iron corrosion inhibition.
- The type of inhibition recorded by the molecule is physisorption
- The molecule exhibits sp^2 hybridization with a lot of p-orbital character on the surfaces of Al(110) and Fe(110); hence, its angles on the surface range between ±0 and ±180

References

1. E. Kroke, C. Posern, C.C. Höhne, U. Böhme, C. Vogt, Synthesis of Thiocyameluric Acid C6N7S3H3, its Reaction to Alkali Metal Thio¬cyamelurates and Organic Tris(dithio)cyamelurates, Chemistry-A European Journal, **2019**, 25, 15555-15564.
2. S. Hong, W. Chen, Y. Zhang, H.Q. Luo, M. Li, N.B. Li, Investigation of the inhibition effect of trithiocyanuric acid on corrosion of copper in 3.0wt.% NaCl, Corrosion Science, **2013**, 66, 308–314.
3. W. Chen, S. Hong, B. Xiang, H.Q. Luo, M. Li, N.B. Li, Corrosion inhibition of copper in hydrochloric acid by coverage with trithiocyanuric acid self-assembled monolayers, Corrosion Engineering, Science and Technology, **2013**, 48, 98–107.
4. N.B. Iroha, C.U. Dueke-Eze, T.M. Fasina, V.C. Anadebe, L. Guo, Anticorrosion activity of two new pyridine derivatives in protecting X70 pipeline steel in oil well acidizing fluid: experimental and quantum chemical studies, J. Iran. Chem. Soc., **2021**, 19, 1–16.
5. R. Songbo, G. Ying, K. Chao, G. Song, X. Shanhua, Y. Liqiong, Effects of the corrosion pitting parameters on the mechanical properties of corroded steel, Constr. Build. Mater., **2021**, 272, 121941.
6. B. El Ibrahim, J.V. Nardeli, L. Guo, An overview of corrosion, ACS Symp Ser., **2021**, 1403, 1–19.
7. M. Conradi, Development of mechanical, corrosion resistance, and antibacterial properties of steels, Materials, **2021**, 14, 1–2.
8. K.P. Dahal, J.N. Timilsena, M. Gautam, J. Bhattarai, Investigation on probabilistic model for corrosion failure level of buried pipelines in Kirtipur urban areas (Nepal), J. Fail. Anal. Prev., **2021**, 21, 914–926.
9. M.M. Hanoon, A.M. Resen, A.A. Al-Amiery, A.A.H. Kadhum, M.S. Takriff, Theoretical and experimental studies on the corrosion inhibition potentials of 2-((6-methyl-2-ketoquinolin-3-yl) methylene) hydrazinecarbothioamide for mild steel in 1 M HCl, Prog. Color. Color. Coat., **2021**, 15, 21–33.
10. N.O. Obi-Egbedi, N.D. Ojo, Computational studies of the corrosion inhibition potentials of some derivatives of 1H-imidazo[4,5-F] [1,10] phenanthroline, J. Sci. Res., **2015**, 14, 50–56.
11. F. Iorhuna, M.A. Ayuba, A.T. Nyijime, M. Sani, H. Abdulmumini, J.O. Oyeyode, A Comparative Computational Stimulation Studies on Corrosion Inhibition and Adsorptive Qualities of Coumarin Derivative on Iron, Zinc, Copper and Aluminium, Eurasian J. Sci. Tech., **2024**, 4(1), 44-56.
12. S. Asadi, G.M. Ziarani, The molecular diversity scope of 1,3-indandione in organic synthesis, Mol Divers, **2016**, 20(1), 111–152.
13. F. Iorhuna, M.A. Ayuba, A.T. Nyijime, H. Muhammadjamiu, M. Ibrahim, Comparative Study of Halogen Substituted Isocyanatophosphine as an Adsorptive Inhibitor on Al (110) Crystal Surface, UsingDensity Functional Theory, Prog. Chem. Biochem. Res, **2023**, 6(3), 211-228.
14. I.B. Obot, D.D. Macdonald, Z.M. Gasem, Density functional theory (DFT) as a powerful tool for designing new organic corrosion inhibitors, Corros. Sci., **2015**, 99, 1–30.

15. A. Dehghani, G. Bahlakeh, B. Ramezanzadeh, A.H. Mostafatabar, Construction of a zinc-centered metal–organic film with high anti-corrosion potency through covalent-bonding between the natural flavonoid-based molecules (Quercetin)/divalent-zinc: Computer modeling (integrated-DFT&MC/MD)/electrochemical-surface assessments, J. Ind. Eng. Chem., **2020**, 88, 382–395.
16. N.S. Abdelshafi, M.A. Sadik, A.M. Shoeib, S.A. Halim, Corrosion inhibition of Aluminum in 1 M HCl by novel pyrimidine derivatives, EFM measurements, DFT calculations and MD simulation, Arab. J. Chem., **2022**, 15(1), 103459.
17. A. Abdullahi Muhammad, N. Aondofa Thomas, N. Usman Shehu, F. Iorhuna, Exploring the Inhibition Potential of Carbamodithionic acid on Fe (111) Surface: A Theoretical Study, J. Eng. Ind. Res., **2024**, 4(4), 201-210.
18. B. El Ibrahimi, A. Jmiai, K. El Mouaden, R. Oukhrib, A. Soumoue, S. El Issami, L. Bazzi, Theoretical evaluation of some α-amino acids for corrosion inhibition of copper in acidic medium: DFT calculations, Monte Carlo simulations and QSPR studies, J. King Saud Univ. Sci., **2020**, 32, 163–171.
19. M.E. Mashuga, L.O. Olasunkanmi, H. Lgaz, E.S.M. Sherif, E.E. Ebenso, Aminomethylpyridazine isomers as corrosion inhibitors for mild steel in 1 M HCl: Electrochemical, DFT and Monte Carlo simulation studies, J. Mol. Liq., **2021**, 344, 117882.
20. R. Hsissou, F. Benhiba, O. Dagdag, M. El Bouchti, K. Nouneh, M. Assouag, A. Elharfi, Development and potential performance of prepolymer in corrosion inhibition for carbon steel in 1.0 M HCl: outlooks from experimental and computational investigations, J. Colloid Interface Sci., **2020**, 574, 43–60.
21. V.S. Sastri, M. Elboujdaini, J.R. Perumareddi, Utility of quantum chemical parameters in the rationalization of corrosion inhibition efficiency of some organic inhibitors, Corrosion, **2005**, 61, 933–942.
22. T. A. Nyijime , H. F. Chahul, P. I. Kutshak, A. M. Ayuba, F. Iorhuna, V. Okai, and A. Hudu. Theoretical Investigation of Aluminum Corrosion Inhibition Using Chalcone Derivatives. Mediterranean Journal of Chemistry 2024, 14(1), 58-68. DOI: http://dx.doi.org/10.13171/mjc02402281774nyijime.
23. N. Hossain, M.A. Chowdhury, M. Kchaou, An overview of green corrosion inhibitors for sustainable and environment friendly industrial development, J. Adhes. Sci. Technol., **2021**, 35, 673–690.
24. Y. Qiang, L. Guo, H. Li, X. Lan, Fabrication of environmentally friendly Losartan potassium film for corrosion inhibition of mild steel in HCl medium, Chem. Eng. J., **2021**, 406, 126863.
25. M. Palomar-Pardavé, M. Romero-Romo, H. Herrera-Hernández, M.A. Abreu-Quijano, N.V. Likhanova, J. Uruchurtu, J.M. Juárez-García, Influence of the alkyl chain length of 2-amino 5 alkyl 1,3,4 thiadiazole compounds on the corrosion inhibition of steel immersed in sulfuric acid solutions, Corros. Sci., **2012**, 54, 231–243.
26. S. Hadisaputra, A.A. Purwoko, S. Hamdiani, Substituents effects on the corrosion inhibition performance of pyrazolone against carbon steels: quantum chemical and Monte Carlo simulation studies, Int. J. Corros. Scale Inhib., **2021**, 10, 419–440.
27. J.D. Pietrzyk, C.W. Frank, Analytical Chemistry, Academic Press, **1979**, 410-424. https://doi.org/10.1016/B978-0-12-555160-1.50022-8.
28. J.S. Amoko, O.F. Akinyele, O.E. Oyeneyin, D.S. Olayanju, Corrosion inhibitive potentials of (E)-5-((4-Benzoylphenyl) Diazenyl)-2-hydroxybenzoic acid on mild steel surface in 0.5 M HCl-experimental and DFT calculations, J Turkish Chem Soc Sect A Chem., **2021**, 8(1), 343–362.
29. J.I. Martinez-Araya, Why is the dual descriptor a more accurate local reactivity descriptor than Fukui functions?, J. Math. Chem., **2015**, 53(2), 451–465.
30. E.O. Oluwatoba, N.D. Ojo, N. Ipinloju, E.B. Agbaffa, A.V. Emmanuel, Investigation of the corrosion inhibition potentials of some 2-(4-(substituted) arylidene)-1H-indene-1,3-dione derivatives: density functional theory and molecular dynamics simulation, Beni-Suef. Univ. J. Basic. Appl. Sci., **2022**, 11, 132
31. M.B. Oulhaoua, M. El Hafi, S. Zehra, L. Eddaif, A.A. Alrashdi, S. Lahmidi, L. Guo, J.T. Mague, H. Lgaz, Colloids and Surfaces A : Physicochemical and Engineering Aspects Synthesis, structural analysis and corrosion inhibition application of a new indazole derivative on mild steel surface in acidic media complemented with DFT and MD studies, Colloids Surf A Physicochem Eng Asp., **2021**, 617, 126373.
32. H. Lgaz, S. Masroor, M. Chafiq, M. Damej, A. Brahmia, R. Salghi, M. Benmessaoud, I.H. Ali, M.M. Alghamdi, A. Chaouiki, I.M. Chung, Evaluation of 2-mercaptobenzimidazole derivatives as corrosion inhibitors for mild steel in hydrochloric acid, Metals, **2020**, 10(3),1–14.
33. A. Zarrouk, B. Hammouti, T. Lakhlifi, M. Traisnel, H. Vezin, F. Bentiss, New 1H-pyrrole-2,5-dione derivatives as efficient organic inhibitors of carbon steel corrosion in hydrochloric acid medium: electrochemical, XPS and DFT studies, Corros. Sci., **2015**, 90, 572–584.

34. O. Oyeneyin, D. Akerele, N. Ojo, O. Oderinlo, Corrosion inhibitive potentials of some 2H–1-benzopyran-2-one derivatives- DFT calculations Biointerface, Res. Appl. Chem., **2021**, 11(6), 13968–13981.
35. F. Iorhuna, A.M. Ayuba, S.A. Minjibir, T.A. Nyijime, A. Ishaq, Adsorptive properties of 4-Hexyl-tertrahydro-thiopyran-1,1- diode on Al(110) and Fe(111) surface using DFT method, Alger. J. Eng. Technol., **2023**, 8(2), 309-315.
36. S. Hadisaputra, A. Abhi Purwoko, A. Hakim, N. Prasetyo, S. Hamdiani, Corrosion Inhibition Properties of Phenyl Phthalimide Derivatives against Carbon Steel in the Acidic Medium: DFT, MP2, and Monte Carlo Simulation Studies, ACS Omega, **2022**, 7(37), 33054–33066.
37. D.M. Jamil, A.K. Al-Okbi, S.B. Al-Baghdadi, A.A. Al-Amiery, A. Kadhim, T.S. Gaaz, A.B. Mohamad, Experimental and theoretical studies of Schiff bases as corrosion inhibitors, Chem. Cent. J., **2018**, 12, 7.
38. A. Kokalj, On the alleged importance of the molecular electron-donating ability and the HOMO–LUMO gap in corrosion inhibition studies, Corros. Sci., **2021**, 180, 109016.
39. M. Rbaa, M. Galai, A.S. Abousalem, B. Lakhrissi, M.E. Touhami, I. Warad, A. Zarrouk, Synthetic, spectroscopic characterization, empirical and theoretical investigations on the corrosion inhibition characteristics of mild steel in molar hydrochloric acid by three novel 8-hydroxyquinoline derivatives, Ionics, **2020**, 26(1), 503–522.
40. N.O. Eddy, E.E. Ebenso, Quantum chemical studies on the inhibition potentials of some *Penicillin* compounds for the corrosion of mild steel in 0.1 M HCl, J. Mol. Model., **2010**, 16, 1291–1306.
41. A.A. Siaka, N.O. Eddy, S.O. Idris, L. Magaji, Z.N. Garba, I.S. Shabanda, Quantum Chemical Studies of Corrosion Inhibition and Adsorption Potentials of Amoxicillin on Mild Steel in HCl Solution, International Journal of Modern Chemistry, **2013**, 4(1), 1-10
42. C.B. Erma, M.A. Quraishi, E.E. Ebenso, I.B. Obot, A. El Assyry, 3-amino alkylated indoles ascorrosion inhibitors for mild steel in 1M HCl: Experimental and theoretical studies, Jour-nal of Molecular Liquids, **2016**, 219, 647-660
43. A. Tazouti, N. Errahmany, M. Rbaa, M. Galai, Z. Rouifi, R. Touir, A. Zarrouk, S. Kaya, M.E. Touhami, B. El Ibrahimi, S. Erkan, Effect of hydrocarbon chain length for acid corrosion inhibition of mild steel by three 8-(n-bromo-Ralkoxy) quinoline derivatives: experimental and theoretical investigations, J. Mol. Struct., **2021**, 1244, 1–19.
44. A.M. Ayuba, N.A. Thomas, N.U. Shehu, F. Iorhuna, Exploring the Inhibition Potential of Carbamodithionic acid on Fe (111) Surface: A Theoretical Study, J. Eng. Ind. Res., **2024**, 4(4), 201-210.
45. M.E. Belghiti, S. Echihi, A. Dafali, Y. Karzazi, M. Bakasse, H. Elalaoui-Elabdallaoui, L.O. Olasunkanmi, E.E. Ebenso, M. Tabyaoui, Computational simulation and statistical analysis on the relationship between corrosion inhibition efficiency and molecular structure of some hydrazine derivatives in phosphoric acid on mild steel surface, Applied Surface Science, **2019**, 491, 707-22.
46. D. Llache Robledo, B. Berner Perez, A.G. Gonzales Guiterrez, R. Flores-Moreno, N. Casillas, DFT as a tool for predicting corrosion inhibition capacity, ECS Trans., **2021**, 101(1), 277–290.
47. A. Singh, K.R. Ansari, P. Banerjee, M. Murmu, M.A. Quraishi, Y. Lin, Corrosion inhibition behavior of piperidinium based ionic liquids on Q235 steel in hydrochloric acid solution: experimental, density functional theory and molecular dynamics study, Colloids Surfaces A Physicochemical Eng. Asp., **2021**, 623, 1–12.
48. A.A. Muhammed, F. Iorhuna, T.A. Nyijime, H. Muhammadjamiu, M. Sani, Exploring 4-Aminnaphthalene Derivatives for Corrosion Inhibition through Density Functional Theory and Simulation on Iron Surface, J. Eng. Ind. Res., **2024**, 5(1), 1-15.